IEEE Access
Multidisciplinary ⋮ Rapid Review ⋮ Open Access Journal

Received 6 September 2023, accepted 10 September 2023, date of publication 22 September 2023,
date of current version 27 September 2023.

Digital Object Identifier 10.1109/ACCESS.2023.3318009

RESEARCH ARTICLE

Phase Error Calculation Caused by Start-Stop Approximation in Processing FMCW Radar Signals for SAR Imaging

VIET T. VU, (Senior Member, IEEE), YEVHEN IVANENKO, (Member, IEEE), AND MATS I. PETTERSSON, (Senior Member, IEEE)
Blekinge Institute of Technology, 37179 Karlskrona, Sweden

Corresponding author: Viet T. Vu (viet.thuy.vu@bth.se)

This work was supported in part by the ELLIIT Research Environment through the Project Multistatic High-Resolution Sensing at THz under Grant A17; and in part by the Crafoord Foundation, Sweden, (“Crafoordska stiftelsen”) under Project 20230898.

ABSTRACT The current synthetic aperture radar (SAR) image formation algorithms have been developed for pulse radar systems, and they are desired for use in for frequency-modulated continuous wave (FMCW) radar systems. Since there is a difference between the outputs of pulse radar and FMCW radar, it is necessary to adapt these algorithms to the output of the pulse radar. In addition, the start-stop approximation, which can be used for the signal processing of pulse radar systems, should be taken into account for FMCW radar systems because the pulse duration of the pulse radar is relatively small in comparison to the modulation time of the FMCW radar. In this study, the phase error caused by the start-stop approximation in processing the data measured by an FMCW radar system for synthetic aperture imaging is investigated. The important results of this study indicate that the start-stop approximation is valid for processing FMCW SAR data in many cases. If the following circumstances occur simultaneously, such as a high radar signal frequency, long modulation time, high platform speed, and short propagation range, then the approximation may become invalid. The simulations and experiments performed with a wideband 154 GHz FMCW radar support this statement.

INDEX TERMS FMCW, ramp duration, phase error, back-projection.

I. INTRODUCTION

Synthetic aperture radar (SAR) is a radar technique that synthesizes large apertures based on the movement of the radar platform. The synthesized aperture is usually much larger than the physical radar aperture. This radar technique has been used for a wide range of applications, such as change detection and ground moving target indication (GMTI), but the most fundamental and important application of SAR is synthetic aperture imaging. The SAR image of a ground scene is reconstructed with measured radar data and by different algorithms that carry out range compression and azimuth compression. The algorithms in the literature have mainly been developed for pulse radar systems using chirp signals and where the start-stop approximation is assumed, for example, the FFT-based class [1], [2], [3], [4] and the back-projection class [5], [6], [7], [8]. This assumption is valid because the speed of an SAR platform, e.g., airborne, is relatively small in comparison with the speed of the wave propagation and the pulse duration is relatively short.

With the emergence of FMCW radar systems and the implementation of the SAR principle on FMCW radar, the algorithms, which were developed for pulse radar systems, are expected to be used for FMCW radar systems. From a mathematical point of view, it is possible to adapt these algorithms to the output of an FMCW radar system. The output of an FMCW radar is intermediate frequency (IF) signals in which the slope of the ramp affects both the linear and quadrature terms of the IF signal in the time domain that will be discussed in Section II-A, with more

The associate editor coordinating the review of this manuscript and approving it for publication was Wei Wang.

details provided (3). However, the effect of the slope of the ramp on the linear term can be moved into the signal envelope by a transformation of the IF signal to the frequency domain that can be done by applying the Fourier transform (FFT) to the IF signal (more details can be found in (4) in Section II-B). By doing this, we can directly obtain the range-compressed signal in which the radar range is achieved with the beat frequency (range time delay scaled with the slope). Therefore, the range compression step in the algorithms developed for the pulse radar systems should be removed and replaced by the phase correction step. However, the question regarding the start-stop approximation due to the long modulation time of the ramp under the realization of the SAR principle for FMCW radar systems has been raised in several publications. In [9], it is shown that the main effect is the Doppler frequency shift that can be compensated by modifying the range migration compensation. However, the simulation results based on a 35 GHz FMCW radar system [10] show that this effect is insignificant. In [11], a signal model was proposed to address the effects caused by a long modulation time presented by an additional range-azimuth coupling term and a range walk term. However, simulations and the test based on Ka-band FMCW radar [12], [13] have not clearly shown the effects. In [14], a rail-based near-field FMCW SAR experiment is presented in which the modulation time and speed of the platform are selected as variables while the output function is the SAR image. The experiment gives us a clear view about the effects when the SAR principle is utilized in FMCW radar systems. In [15], two back-projection algorithms, the standard algorithm based on the start-stop approximation and a modified version that considers the movement of the sensor during the modulation time, are developed and examined with numerical simulations, showing that the start-stop approximation is not always valid for FMCW SAR. However, a metric that is used to measure such effects, e.g., the phase error, can provide a better view of the validity of the start-stop approximation for FMCW SAR. Moreover, it is necessary to examine the start-stop approximation with the practical FMCW SAR systems.

The aim of this study is to investigate the phase error in processing the data measured by an FMCW radar system in synthetic aperture imaging when the modulation time of the ramp is ignored. The phase error will define the limits on the speed and modulation time. The contribution of this study is the formula that can be used to estimate the phase error caused by start-stop approximations for FMCW SAR. It is a function of the radar signal frequency, radar range, modulation time of the FMCW radar system and platform speed. Based on this formula, we can state that the start-stop approximation is valid for processing FMCW SAR data in many cases. This approximation is invalid if a high radar signal frequency, long modulation time, high platform speed, and short propagation range occur sumultaneously. This statement is supported by the simulations and the experiments performed with a wideband 154 GHz FMCW radar.

The rest of the paper is organized as follows: In Section II, the operation of an FMCW radar is presented. For an FMCW radar, the range is compressed by transforming the IF signal of FMCW radar to the frequency domain. The aperture is synthesized for an FMCW radar by mounting it on a platform. In Section III, we reviewed some FMCW radar systems used for synthesizing the aperture and calculated the phase error in SAR processing of the signals measured by these systems. In Section IV, some simulation results are presented. They show the effects of the start-stop approximation that occur in the region where it can almost or no longer be valid. The experimental results based on a wideband 154 GHz FMCW radar are provided in Section V. Finally, in Section VI, concluding remarks are provided.

II. FMCW SAR

In this section, we provide a short discussion of FMCW SAR based on an FMCW radar system. Some practical issues are also addressed.

A. FMCW RADAR

For an FMCW radar, the phase of the transmitted complex linear frequency-modulated chirp signal in the radio frequency (RF) domain can be expressed by

$$\phi_{TX}(\tau) = \exp\left\{j2\pi\nu_{min}\tau + j\pi\kappa\tau^2\right\}, 0 \le \tau \le T \quad (1)$$

where τ denotes range time. The start frequency of the emitted ramp is ν_{min} with the modulation time T, and the slope of the emitted ramp is κ. The emitted ramp is assumed to propagate in a homogeneous medium and is reflected by a scatterer. The reflection by the scatterer is detected by the receiver afterward. If there exists a scatterer located at the radar range R, the phase of the received signal for the given azimuth time t in the RF domain will be expressed by

$$\phi_{RX}(t,\tau) = \exp\left\{j2\pi\nu_{min}\left(\tau - \frac{2R}{c}\right) + j\pi\kappa\left(\tau - \frac{2R}{c}\right)^2\right\} \quad (2)$$

where c is the speed of propagation. The received signal in the RF domain is then down-converted in the intermediate frequency (IF) domain. This ensures that the signal can be sampled properly. The down-conversion can be implemented by mixing the transmitted and received signals. The phase of the output of the mixer is derived by

$$\phi_{IF}(t,\tau) = s_{TX}(\tau)\,\bar{s}_{RX}(t,\tau) = \exp\left\{j2\pi\left(\nu_{min} + \kappa\tau\right)\frac{2R}{c} - j\pi\kappa\left(\frac{2R}{c}\right)^2\right\} \quad (3)$$

where $\nu(\tau) = \nu_{min} + \kappa\tau$ denotes the linear modulated frequency of the chirp.

Equation (3) shows that the mathematical expression of the IF signal at the output of a FMCW radar is similar to that of a pulse radar except for the slope of FMCW radar (the chirp rate of pulse radar) κ in the linear term of the exponential function.

B. RANGE COMPRESSION

Range compression is achieved by applying the Fourier transform to the IF signal. This can be proven as follows:

$$\begin{aligned} & S_{IF}(t, \nu) \\ &= \int_{-\infty}^{\infty} s_{IF}(\tau) \exp\{-j2\pi\nu\tau\}\, d\tau \\ &= \exp\left\{\frac{j4\pi\nu_{min}R}{\mathrm{c}} - j\pi\kappa\left(\frac{2R}{\mathrm{c}}\right)^2\right\} \\ &\quad \times \int_{-\infty}^{\infty} w(\tau) \exp\left\{j2\pi\left(\kappa\frac{2R}{\mathrm{c}}\right)\tau\right\} \exp\{-j2\pi\nu\tau\}\, d\tau \\ &= W\left(\nu - \kappa\frac{2R}{\mathrm{c}}\right) \exp\left\{\frac{j4\pi\nu_{min}R}{\mathrm{c}} - j\pi\kappa\left(\frac{2R}{\mathrm{c}}\right)^2\right\} \end{aligned} \tag{4}$$

where $w(\tau)$ is the envelope of the IF signal and $W(\nu)$ is the range compressed envelope in the ν domain, obtained by the Fourier transform of $w(\tau)$. If $w(\tau)$ is a rectangular window, then $W(\nu)$ is a sinc function, and if $w(\tau)$ is a tapered window, $W(\nu)$ is a sinc-like function with a lower sidelobe. The frequency shift defines a beat at

$$\nu_b = \kappa\frac{2R}{\mathrm{c}} \tag{5}$$

showing the relationship between the range R and the beat frequency ν_b. We can also rewrite (5) using the ramp duration T and the sweep bandwidth B as

$$\nu_b = \frac{B}{T}\frac{2R}{\mathrm{c}} \Leftrightarrow R = \frac{\mathrm{c}T}{2}\frac{\nu_b}{B} \tag{6}$$

After the phase correction, the exponential terms in (4) will be eliminated. In practice, the quadratic term in the exponent of (4) can be neglected directly for short ranges, R. If we change the frequency variable ν to a time variable and convert the beat frequency ν_b to the radar range R, we obtain the range compressed signal.

C. SYNTHESIZING APERTURE FOR FMCW RADAR AND START-STOP APPROXIMATION

To realize the SAR principle for FMCW radar, an FMCW radar is mounted on a platform, e.g., a car for automotive SAR applications or a drone for SAR surveillance applications. The platform continuously moves with speed v while the radar performs the measurements. A platform can be an unmanned aerial vehicle (drone), a ground vehicle or an aircraft. The duty cycle of FMCW SAR is the time separation between two ramps and is defined by $T + \Delta T$, where T is the modulation time of the ramp and ΔT is the delay until the next ramp. The conditions for the duty cycle can be expressed as

$$\frac{\mathrm{c}}{4\nu_c} \le v(T + \Delta T) \le \frac{\mathrm{c}}{2\nu_{\max}\sin(\theta_{\max}/2)} \tag{7}$$

where ν_c and $\nu_{\max}$ are the center frequency and stop frequency of an emitted ramp, and $\theta_{\max}$ is the maximum synthetic angle (integration angle). The lower bound is the condition that ensures that some algorithms can work without γ processing [16]. γ processing is required if the values of the fractional bandwidth and/or integration angle are large, leading to the azimuth wavenumber being larger than two times the range wavenumber. Scaling the speed of the platform with a factor larger than 1 in the γ processing helps to decrease the azimuth wavenumber below the limit (two times the range wavenumber). The upper bound comes from the condition that the inversion of the duty cycle should be larger than two times the maximum Doppler frequency.

If t_0 is the time instance where the FMCW radar starts transmitting a ramp, then the time instance when the FMCW radar receives the reflection from an object at the radar range R is $t_0+T+\tau_0$, where $\tau_0 = 2R/\mathrm{c}$ is the range time delay. Since the speed of an SAR platform is small in comparison to the speed of the wave propagation, the following approximation $t_0 + T + \tau \approx t_0 + T$ holds.

For a pulsed radar, the pulse duration of the chirp signal (similar to the modulation time of the ramp T) is relatively short, e.g., on the order of sub-μs, and we can further approximate $t_0 + T \approx t_0$. This is known as the start-stop approximation and a standard signal processing approach for SAR using pulse radar. In this case, the platform is approximately stopped for each measurement, and the phase error caused by this approximation is ignored. For an FMCW radar, the modulation time of the ramp is usually much longer, e.g., on the order of sub-ms. If we consider that the aperture position corresponds to the time instance t_0 and apply the start-stop approximation, the phase error caused by this approximation will be estimated by

$$|\Delta\phi| = \frac{2\pi}{\lambda}\left|\sqrt{R^2 + \left(\frac{vT}{2}\right)^2 - RvT\sin\left(\frac{\theta}{2}\right)} - R\right| \tag{8}$$

where λ is the wavelength and $(\pi - \theta)/2$ is the angle formed by the range vector $\vec{R}$ with length R and the platform velocity $\vec{v}$ with the corresponding speed v. Applying the Taylor expansion to the square root term in (8) and due to $vT \ll R$, the maximum phase error is derived by

$$\max|\Delta\phi| = \frac{\pi f_{\max} vT}{\mathrm{c}}\sin\left(\frac{\theta_{\max}}{2}\right) \le \frac{\pi f_{\max} vT}{\mathrm{c}} \tag{9}$$

According to the far-field condition being widely applied in antenna techniques, the effects caused by phase error can be ignored if $\Delta\phi \le \pi/8$ [17]. This leads to the limit of the platform speed so that the start-stop approximation is valid for realizing the SAR principle for FMCW radar

$$v \le \frac{\mathrm{c}}{8 f_{\max} T \sin(\theta_{\max}/2)} \tag{10}$$

We can also rewrite (10) in the form showing the limit of modulation time of ramp

$$T \le \frac{\mathrm{c}}{8 f_{\max} v \sin(\theta_{\max}/2)} \tag{11}$$

TABLE 1. Parameters of FMCW SAR systems.

FMCW SAR	Epsilon-Lambda	MEMPHIS	2π SENSE
Parameters			
Center frequency [GHz]	35	94	154
Bandwidth [GHz]	0.5	0.8	56
Modulation time [ms]	1	$4 \cdot 10^{-4}$	4.096
Platform speed [m/s]	25	65	0.04876
Radar range [m]	730	812	2
Aperture length [m]	25	1.365	0.235
Calculations			
Integration angle [rad]	$3.5 \cdot 10^{-2}$	$1.7 \cdot 10^{-3}$	$1.2 \cdot 10^{-1}$
Phase error [rad]	$1.6 \cdot 10^{-1}$	$2.2 \cdot 10^{-5}$	$2.2 \cdot 10^{-2}$
Limits			
Speed [m/s]	61	$1.2 \cdot 10^{6}$	$8.6 \cdot 10^{-1}$
Modulation time [ms]	2.4	7.2	72

or even in the form showing the limit of radar range

$$R \geq \frac{8 f_{\max} v T L}{\mathrm{c}} \tag{12}$$

where L denotes the synthetic aperture.

It is important to highlight that, in addition to the condition given in (7), the duty cycle of FMCW SAR should be larger than or equal to the sum of the modulation time of the ramp and the range time delay, i.e., $T + \tau_0$.

III. PRACTICAL FMCW SAR SYSTEMS

In this section, we investigate the phase errors caused by ignoring the modulation time in FMCW SAR processing for several practical FMCW SAR systems.

A. SYSTEM PARAMETERS

The first part of Table 1 summarizes the parameters of three different FMCW SAR systems. The first system is an FMCW SAR demonstrator system with an FMCW radar system manufactured by EPSILON-LAMBDA Electronics that is mounted on a Stemme SI0 glider [9], [10]. The second system is the FHR's airborne millimeter-wave SAR system (MEMPHIS) carried by the Transall C-160 aircraft [11], [12], [13]. The third system is the experimental sub-THz SAR system built on 2πSENSE, a wideband 154 GHz FMCW radar [18]. The radar system is mounted on the moving track of the print head of a 3D printer.

B. PHASE ERROR CALCULATION AND ANALYSIS

The phase error equation (9) requires $\theta_{\max}$ for calculation. It is nothing else than the maximum integration angle that a SAR system can synthesize and calculates by

$$\sin\left(\frac{\theta_{\max}}{2}\right) = \frac{L}{2\sqrt{(L/2)^2 + R^2}} \approx \frac{L}{2R} \tag{13}$$

where L is the length of the synthetic aperture. With the given ranges and the given aperture lengths in Table 1, the maximum integration angles of the considered systems are retrieved and given in the second part of Table 1. Based on these values, we can calculate the phase errors caused by applying the start-stop approximation in SAR processing for FMCW radar systems using (9). The calculated results show that the phase errors caused by the start-stop approximation are in the range that the effects caused by phase error are negligible, i.e., still below the limit $\Delta\phi \leq \pi/8$. In particular, for MEMPHIS, the phase errors are extremely small.

We can see that although the operating frequency range and the platform speed of MEMPHIS are approximately three times higher than those of Epsilon-LAMBDA, the modulation time and the synthesis aperture are short, resulting in an extremely small phase error. In the opposite case, the long modulation time and the long synthesis aperture will not result in a large phase error due to the low operating frequency range and the low platform speed of Epsilon-LAMBDA. For 2π SENSE, due to the extremely low speed of the platform, the phase error is also small despite the high frequency and long modulation time. Hence, a large phase error can only be reached if and only if the following circumstances occur simultaneously: a high operating frequency range, high platform speed, long modulation time and long synthesis aperture. In other words, the start-stop approximation is valid for processing FMCW SAR data for many cases, and it is not always necessary to take into account the problem caused by the start-stop approximation.

C. LIMITS FOR THE VALIDITY OF THE START-STOP APPROXIMATION

In the third part of Table 1, the limits on the platform speed that ensure the start-stop approximation is valid for processing FMCW SAR data are provided. To estimate the speed limits, the parameters of the FMCW radars are maintained and inserted into (10), providing upper limits for speed. For the Epsilon-Lambda system, the limit for speed is 61 m/s, which is approximately the glider's maximum cruise speed (62 m/s). For MEMPHIS, the limit for speed is on the order of 10^6 m/s. Reaching such a speed limit is unfeasible for any aircraft.

The wideband 154 GHz FMCW radar is a sub-THz system that suffers from high atmospheric absorption. This limits the propagation range so that the system is only suitable for short detection range applications or indoor applications. The platforms that are suitable for THz FMCW radar for implementing SAR can be ground-based linear tracks, ground vehicles and unmanned aerial vehicle drones. For indoor measurements with a radar range of 2 m, a high-speed platform for the radar system is unsuitable. The limit of the

TABLE 2. Simulation parameters.

Parameter	Case 1	Case 2	Case 3	Case 4
Duty cycle [ms]	1			
PRF [Hz]	1000			
Speed [m/s]	0	60	120	240
Aperture step [mm]	240	60	120	240
Aperture positions	104	416	208	104
Phase error [rad]	0	$\approx \pi/8$	$\approx \pi/4$	$\approx \pi/2$

platform speed of 8.6×10^{-1} m/s is approximately twenty times the speed of the print head of a 3D printer.

Now, if we assume that the speeds of the platform are unchanged, it is possible to change the slope of the emitted ramp κ to modify the modulation time of the FMCW radar systems. Then, the upper limits for modulation time can be retrieved with (11). In the third part of Table 1, the calculated limits on modulation time are reported.

IV. SIMULATION RESULTS

In this section, we investigate the effects caused by phase errors based on the simulations. The parameters of EPSILON-LAMBDA will be considered for the simulations, as the system suffers from the largest phase error among the considered systems.

A. SIMULATION PARAMETERS

Except the speed of the platform, all parameters of EPSILON-LAMBDA are maintained unchanged. By modifying the speed of the platform, we can obtain different phase errors and observe the effects caused by the phase errors. Other variations that result in the same effects are the modifications of the operating frequency range, the modulation time and integration angle. However, these modifications are not considered in the simulations. For the modulation time of 1 ms, the maximum pulse repetition frequency (PRF) will be 1000 Hz, and this value is used to set the other motion parameters of the platform.

The ground scene is simulated by a point-like scatterer located in the center. The radar range and the aperture length are identical to the arrangement of the Stemme SI0 glider, but the speed of the simulated platform can be set by $[60, 120, 240]$ m/s, corresponding to the phase errors of $[\pi/8, \pi/4, \pi/2]$ radians. For the reference, the platform speed of 0 m/s, i.e., the platform is completely stationary during the radar measurements, is also considered in the simulation. In this case, there is no phase error, and no start-stop approximation is needed during processing. It is worth mentioning that modifying the platform speed over a wide range is impractical for SAR systems built on FMCW radar. For example, we can obtain the platform speed of 0 m/s with linear tracks controlled by a step motor, but such linear tracks cannot provide movements with a speed of 240 m/s.

Different platform speeds will result in different aperture steps and, hence, different numbers of aperture positions. For the speeds $[60, 120, 240]$ m/s, the aperture steps are $[60, 120, 240]$ mm, respectively, and the number of aperture positions are $[416, 208, 104]$. For a platform speed of 0 m/s, the number of aperture positions is selected as 104. The parameters for the simulations are summarized in Table 2, and the simulations are named Case 1, Case 2, Case 3, and Case 4.

B. SAR IMAGE FORMATION

The SAR images are reconstructed from the acquired IF signal matrices using the back-projection algorithm [5], [6]. We consider the slant range plane as the defined image plane. After performing the Fourier transform for the IF signal matrices in range, we obtain the range compressed data matrices $S_{IF}(t, \nu)$, where the azimuth time t and the radar frequency ν refer to the aperture positions and the radar ranges, respectively.

The back-projection algorithm for image reconstruction is based on the shift and superposition of the range compressed data. If we use an integral to represent the superposition, then the back-projection algorithm can be expressed by

$$\Im(\xi, \rho) = \int_{-t_0/2}^{t_0/2} S_{IF}\left(t, \nu - \kappa\frac{2\tilde{R}}{c}\right) \exp\left\{\frac{-j4\pi\nu_{min}\tilde{R}}{c}\right\} dt \tag{14}$$

where t_0 is the integration time and $\tilde{R}$ is the range distance calculated for the aperture position defined by vt and a given azimuth ξ and range ρ in the defined image plane

$$\tilde{R} = \sqrt{(vt - \xi)^2 + \rho^2}. \tag{15}$$

Notably, for short radar ranges, the quadratic term in (4) can be neglected. Only the linear term is considered in the back-pojection algorithm. It is common knowledge that $\tilde{R}$ may not correspond to a range sample of $S_{IF}(t, \nu)$. Therefore, the back-projection algorithm is always associated with an interpolator. It is assumed that $(R_k, S_{IF}(t, \nu - \kappa 2R_k/c))$, where $1 \le k \le K$ and $K \in \mathbb{Z}$ are the available interpolating points surrounding $(\tilde{R}, S_{IF}(t, \nu - \kappa 2\tilde{R}/c))$. For a weighted truncated sinc interpolator [19], the interpolated complex value will be estimated by

$$\begin{aligned} &S_{IF}\left(t, \nu - \kappa\frac{2\tilde{R}}{c}\right) \\ &= \sum_{k=1}^{K} w_k S_{IF}\left(t, \nu - \kappa\frac{2R_k}{c}\right) \exp\left\{-\frac{j4\pi\nu_{min}R_k}{c}\right\} \\ &\quad \times \exp\left\{\frac{j4\pi\nu_c(\tilde{R} - R_k)}{c}\right\} \operatorname{sinc}\left\{\frac{\pi(\tilde{R} - R_k)}{\Delta\tilde{R}}\right\} \end{aligned} \tag{16}$$

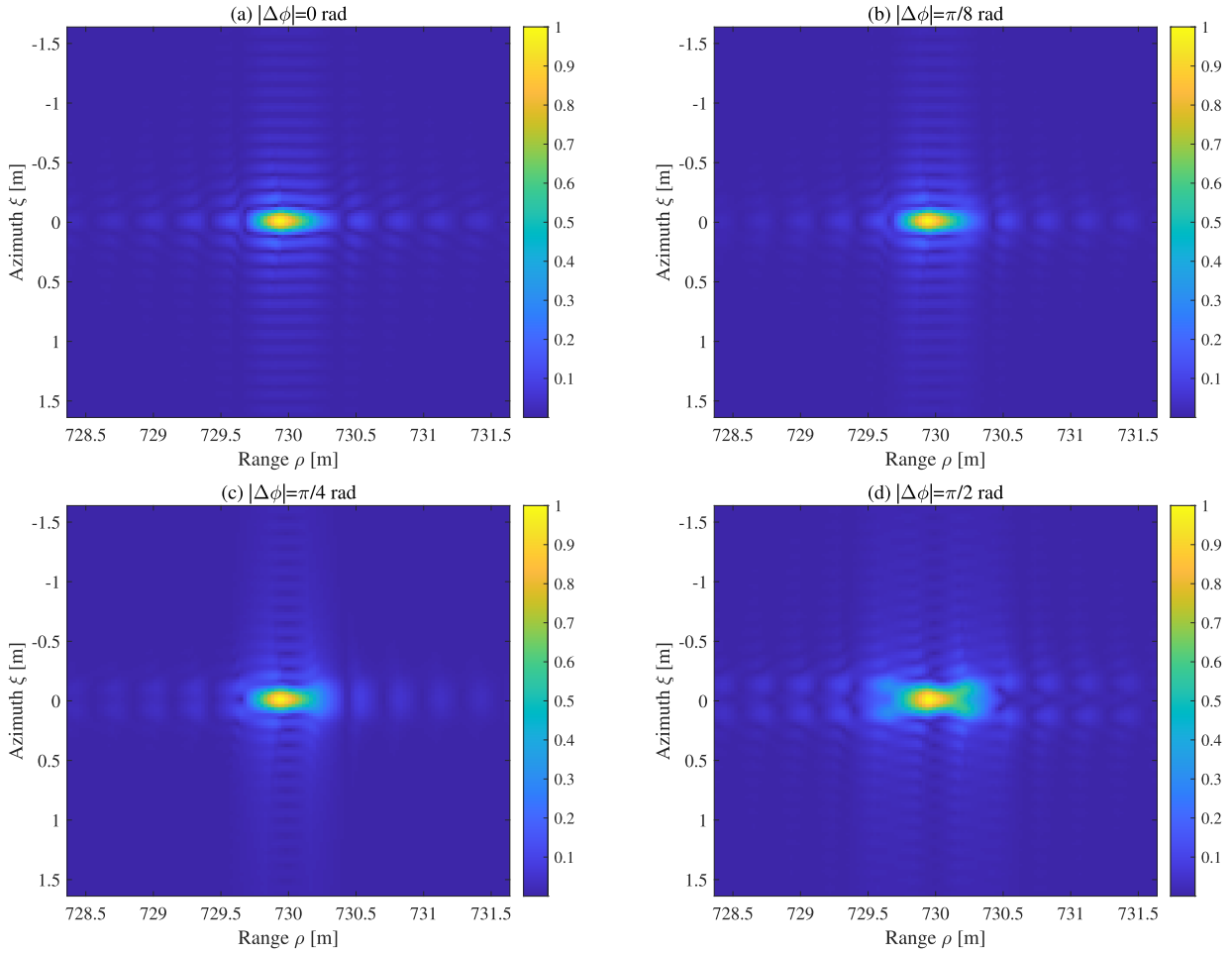

FIGURE 1. SAR images with different phase errors caused by the start-stop approximation. (a) No start-stop approximation and no phase error. (b) Start-stop approximation, in which the effects of the resulting phase error can be neglected. (c) and (d) Start-stop approximations, in which the effects of the resulting phase error cannot be neglected.

where w_k denotes the coefficient of the Hanning window, $\Delta\tilde{R}$ is the difference between two range samples $\tilde{R}$, and ν_c is the center frequency emitted at the fast time $\tau = T/2$. It is obvious that the interpolation procedure takes into account the phase that contains the information regarding the range distance $\tilde{R}$.

Four simulated datasets corresponding to Case 1, Case 2, Case 3 and Case 4 are processed by (16), resulting in four SAR images, as shown in Figure 1. The phase errors caused by the start-stop approximation are ignored during processing.

C. ANALYSIS

The reference SAR image with no phase error is given in Fig. 1(a), and it is visually identical to the SAR image of Fig. 1(b), in which a maximum phase error of $\pi/8$ occurs. No clear difference between the two SAR images can be recognized. It is worth mentioning that the speed corresponding to this phase error is approximately 2.5 times the speed of the practical platform Stemme SI0 glider. The speeds of 120 m/s and 240 m/s used for the next cases are impractical for this platform. For a speed of 120 m/s, the maximum phase error is $\pi/4$. The differences between the SAR images given in Fig. 1(a) and Fig. 1(c) can now be observed. The phase error leads to the smearing of the point target. The smearing is equivalent to the losses in the range and azimuth resolutions and the reduction in the peak intensity of the point target in the image. The larger the phase errors that affect the SAR images, the stronger the smears of of the point target are. This statement is illustrated by the radar image suffering from a maximum phase error of $\pi/2$ as shown in Fig. 1(d). The effects of the phase error can be clearly observed.

The losses in the range and azimuth resolutions can be observed by the half power beamwidth (-3 dB) of the range and azimuth cuts surrounding the peak intensities, respectively. Hence, at the peak intensity of each SAR image given in Fig. 1 (the peak intensity of the point target), we extract a range cut and an azimuth cut, normalize with the peak intensity, and plot them as shown in

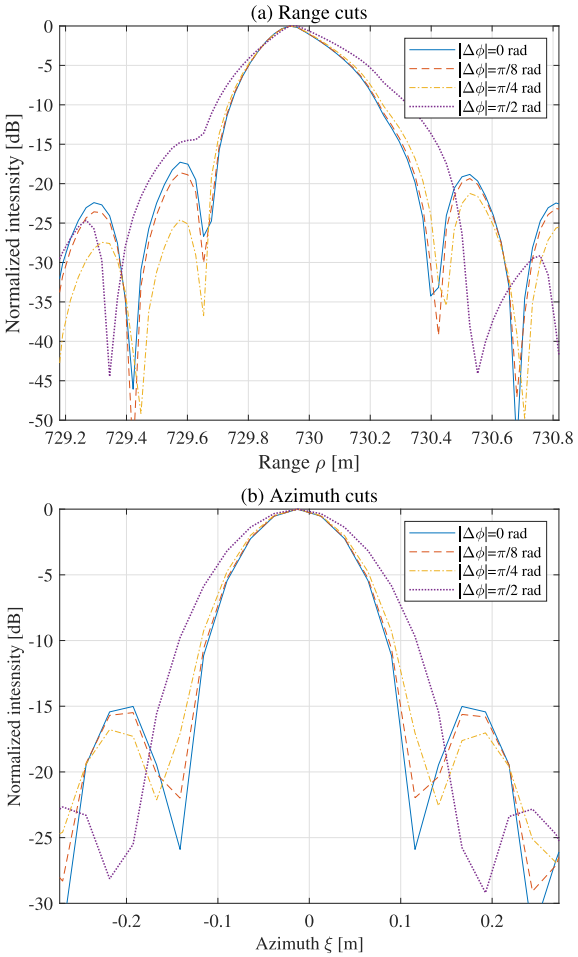

FIGURE 2. (a) Range cuts, (b) azimuth cuts for analysis, extracted from SAR images given in Fig. 1.

TABLE 3. Arrangements for SAR data acquisitions based on 2πSENSE.

Parameters	First acquisition	Second acquisition
Maximum aperture	0.235 m	0.235 m
Minimum range	2 m	2 m
Platform speed	Not applied	0.04876 m/s
Integration angle	8°	8°
Aperture step	2 mm	2 mm
Number of aperture positions	118	118
Duty cycle	41.02 ms	41.02 ms
Modulation time	4.096 ms	4.096 ms
Integration time	Not applied	4.8 s

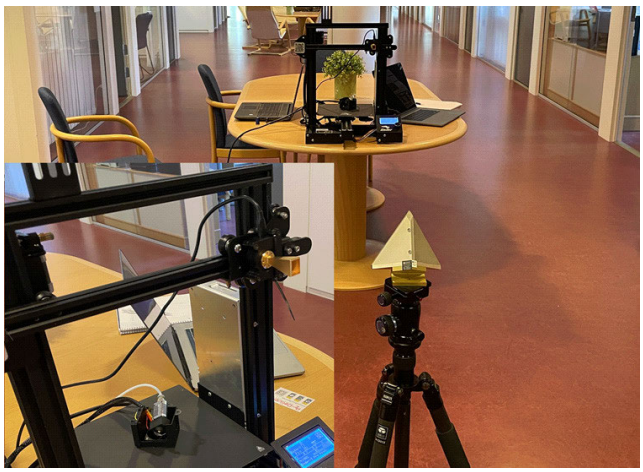

FIGURE 3. Measurement setup.

Fig. 2(a) and Fig. 2(b). The measured range resolutions are $[0.233, 0.234, 0.244, 0.288]$ m corresponding to the phase errors of $[0, \pi/8, \pi/4, \pi/2]$ radians. The loss in the range resolution is approximately 23% for a phase error of $\pi/2$ radians.

V. EXPERIMENTAL RESULTS

To investigate the phase error caused by the start-stop approximation in processing practical FMCW SAR data, we built an SAR system based on a wideband 154 GHz FMCW radar. The parameters of the radar are given in the first part of Table 3. For this investigation, two data acquisitions were conducted. In the first acquisition, the SAR platform completely stops at each aperture position and waits until the FMCW radar finishes the measurement at that position before moving to the next aperture position. In the second acquisition, the platform continuously moves with a constant speed, and the FMCW radar performs the measurements during the movement of the platform. The first acquisition can be considered the ideal case with the start-stop principle resulting in no phase error during processing, whereas the second acquisition can be considered the practical case with phase errors caused by the start-stop approximation during processing. This helps us to examine the validity of the start-stop approximation during processing.

Therefore, it is necessary for the SAR platform to have the capability to move the FMCW radar system along the track with a desired step and with a desired speed. The moving track of the print head of a 3D printer can fulfill the requirements of the SAR platform.

A. ARRANGEMENT

The FMCW radar system is mounted on the moving track of the print head of a 3D printer, as shown in Fig. 3. Hence, the 3D printer will act as a platform, and the system is a ground-based SAR system. The track of the print-head supports the movement of the FMCW radar system along the track with a desired step and with a desired speed. The track allows us to synthesize a maximum aperture of 0.235 m.

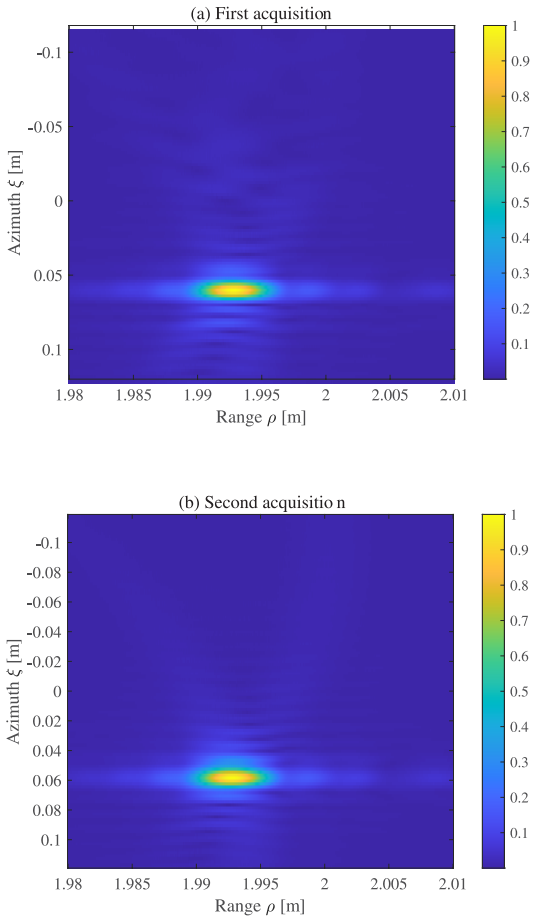

FIGURE 4. SAR images formed by IF signal acquired with: (a) a constant step size of 2 mm; and (b) a constant speed of $v = 48.755$ mm/s.

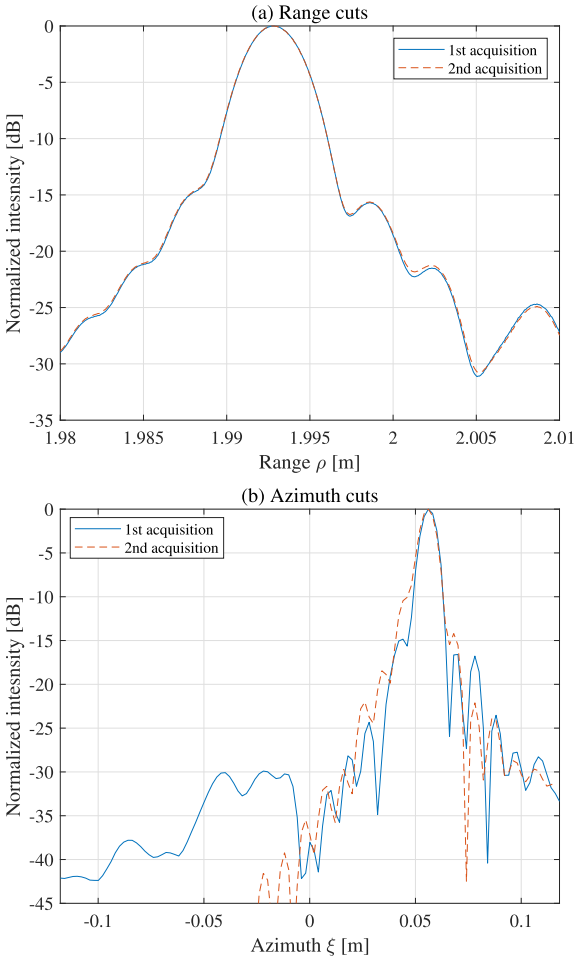

FIGURE 5. (a) Range cuts and (b) azimuth cuts for analysis, which are extracted from the SAR images in Fig. 4.

A corner reflector is placed in front of the radar system with a distance of approximately 2 m. For a maximum aperture, the synthetic angle in this range is approximately $\theta_{max} = 1.2 \times 10^{-1}$ radians. Substituting the available values into (7), the possible range for the aperture step is 4.9×10^{-4} m $\leq \delta \leq 1.2 \times 10^{-2}$ m. An aperture step of $\delta = 2$ mm that lies inside the possible range and can be easily handled by the track is selected for this experiment. We summarize the values in the second column of Table 2.

The data acquisitions are carried out in a normal indoor environment. For the first data acquisition with the start-stop principle, the FMCW radar system is moved to the aperture position with the step $\delta = 2$ mm. It stops at the aperture position, the radar measurements are performed at that aperture position. After data acquisition, we obtain an IF signal matrix with the dimensions of $M \times N$, where $M = 118$ is the total number of aperture positions, and $N = 4096$ is the number of range samples.

For the second data acquisition with the start-stop approximations, the FMCW radar system is moved at a constant speed of 48.755 mm/s. To obtain the same aperture step as the data acquisition without the start-stop approximation, the duty cycle is configured by 41.02 ms, that is, the quotient of the aperture step to the platform speed. Hence, the modulation time is only a tenth of the duty cycle. The integration time is 4.8 s. After the data acquisition, we also obtain an IF signal matrix with the dimensions of 118×4096.

B. EVALUATION

The SAR image formed by the IF signal of the FMCW radar from the data acquisitions with the start-stop principle (no approximation) is provided in Fig. 4(a). The target (corner reflector) is well focused as a point target and at the correct position in the SAR image. It is worth mentioning that there is no phase error in forming the SAR image caused by the start-stop approximation. This image is considered to be the reference for validating the start-stop approximation. The SAR image formed by the IF signal of FMCW radar from the data acquisitions with the start-stop approximation is provided in Fig. 4(b). Compared with the image given in

Fig. 4(a), there is no clear difference between the two SAR images found.

To obtain a better validation for the start-stop approximation, comparing the range and azimuth cuts is reasonable. At the peak intensity of the point target of the SAR image given in Fig. 4(a), we extract a range cut and an azimuth cut, normalize with the peak intensity, and plot them in Fig. 5(a) and Fig. 5(b), respectively. They are the references for validating the start-stop approximation. The same procedure is applied to extract the range and azimuth cuts of the SAR image given in Fig. 4(b). We plot them in the same figures. We can now directly observe the effects of the phase error caused by the start-stop approximation in FMCW SAR processing.

The range cuts given in Fig. 5(a) are identical. There is no difference between the reference range cut and the range cut corresponding to the start-stop approximation. However, there are small differences between the azimuth cuts given in Fig. 5(b). The difference occurs below -10 dB, which does not affect the azimuth resolution that is measured at -3 dB. The difference does not create a higher peak sidelobe. Actually, the sidelobes do not spread far from the main lobe similar to the reference cut. Hence, the phase error caused by the start-stop approximation in processing can be neglected. This partially confirms the conclusion that it is unnecessary to take into account the modulation time in SAR processing for FMCW radar signals in many cases; in other words, the start-stop approximation is valid for processing FMCW SAR data.

VI. CONCLUSION

In this paper, the phase error caused by the start-stop approximation during processing the data measured by an FMCW radar system for synthetic aperture imaging has been studied. Under the assumption of start-stop approximation, the phase errors calculated for the currently used FMCW SAR systems, such as Epsilon-LAMBDA, MEMPHIS and 2πSENSE, are small. The speed limits and modulation time limits are significantly larger than possible values that can be set for these systems in practice. Several simulations with different platform speeds have been used to investigate the effects of the start-stop approximation. Two data acquisitions under different circumstances were also carried out with a wideband 154 GHz FMCW radar, which is a sub-THz system. The main conclusion is that the start-stop approximation is valid for processing FMCW SAR data in many cases; in other words, we can ignore the modulation time T during SAR processing for FMCW radar signals. To avoid the complexity caused by the start-stop approximation, certain circumstances, such as a high radar signal frequency, long modulation time, high platform speed and short propagation range, should be considered in the system design. These circumstances should not occur simultaneously.

ACKNOWLEDGMENT

The authors would like to thank 2π-Labs GmbH for providing the radar system for the research.

REFERENCES

[1] J. R. Bennett and I. G. Cumming, "Digital processor for the production of Seasat synthetic aperture radar imagery," in *Proc. Int. Conf. Seasat-SAR Processor*, Frascati, Italy, Dec. 1979, Paper no. ESA-SP-154.

[2] C. Cafforio, C. Prati, and F. Rocca, "SAR data focusing using seismic migration techniques," *IEEE Trans. Aerosp. Electron. Syst.*, vol. 27, no. 2, pp. 194–207, Mar. 1991.

[3] R. K. Raney, H. Runge, R. Bamler, I. G. Cumming, and F. H. Wong, "Precision SAR processing using chirp scaling," *IEEE Trans. Geosci. Remote Sens.*, vol. 32, no. 4, pp. 786–799, Jul. 1994.

[4] G. W. Davidson, I. G. Cumming, and M. R. Ito, "A chirp scaling approach for processing squint mode SAR data," *IEEE Trans. Aerosp. Electron. Syst.*, vol. 32, no. 1, pp. 121–133, Jan. 1996.

[5] H. Hellsten and L. E. Andersson, "An inverse method for the processing of synthetic aperture radar data," *Inverse Problems*, vol. 3, no. 1, pp. 111–124, 1987.

[6] L.-E. Andersson, "On the determination of a function from spherical averages," *SIAM J. Math. Anal.*, vol. 19, no. 1, pp. 214–232, Jan. 1988.

[7] A. F. Yegulalp, "Fast backprojection algorithm for synthetic aperture radar," in *Proc. IEEE Radar Conf. (RadarCon)*, Waltham, MA, USA, Apr. 1999, pp. 60–65.

[8] L. M. H. Ulander, H. Hellsten, and G. Stenstrom, "Synthetic-aperture radar processing using fast factorized back-projection," *IEEE Trans. Aerosp. Electron. Syst.*, vol. 39, no. 3, pp. 760–776, Jul. 2003.

[9] J. J. M. de Wit, A. Meta, and P. Hoogeboom, "Modified range-Doppler processing for FM-CW synthetic aperture radar," *IEEE Geosci. Remote Sens. Lett.*, vol. 3, no. 1, pp. 83–87, Jan. 2006.

[10] A. Meta, J. J. M. de Wit, and P. Hoogeboom, "Development of a high resolution airborne millimeter wave FM-CW SAR," in *Proc. Eur. Radar Conf. (EuRAD)*, Amsterdam, The Netherlands, Oct. 2004, pp. 209–212.

[11] R. Wang, O. Loffeld, H. Nies, S. Knedlik, M. Hagelen, and H. Essen, "Focus FMCW SAR data using the wavenumber domain algorithm," *IEEE Trans. Geosci. Remote Sens.*, vol. 48, no. 4, pp. 2109–2118, Apr. 2010.

[12] H. Essen, H. Fuchs, and A. Pagels, "High resolution millimeterwave SAR for the remote sensing of wave patterns," in *Proc. IEEE Int. Geosci. Remote Sens. Symp. (IGARSS)*, Barcelona, Spain, Jul. 2007, pp. 963–966.

[13] H. Essen, T. Brehm, M. Hagelen, and H. Schimpf, "Remote sensing at millimetre waves with the MEMPHIS synthetic aperture radar," in *Proc. EUSAR*, Friedrichshafen, Germany, Jun. 2008, pp. 1–4.

[14] M. Wielage, F. Cholewa, P. Pirsch, and H. Blume, "Experimental violation of the start-stop-approximation using a holistic rail-based UWB FMCW-SAR system," in *Proc. VDE EUSAR*, Hamburg, Germany, Jun. 2016, pp. 838–841.

[15] A. Ribalta, "Time-domain reconstruction algorithms for FMCW-SAR," *IEEE Geosci. Remote Sens. Lett.*, vol. 8, no. 3, pp. 396–400, May 2011.

[16] V. T. Vu, T. K. Sjögren, and M. I. Pettersson, "Ultrawideband chirp scaling algorithm," *IEEE Geosci. Remote Sens. Lett.*, vol. 7, no. 2, pp. 281–285, Apr. 2010.

[17] C. A. Balanis, *Antenna Theory—Analysis and Design*, 2nd ed. Hoboken, NJ, USA: Wiley, 1997, p. 33.

[18] J. Schorlemer, C. Schulz, N. Pohl, I. Rolfes, and J. Barowski, "Compensation of sensor movements in short-range FMCW synthetic aperture radar algorithms," *IEEE Trans. Microw. Theory Techn.*, vol. 69, no. 11, pp. 5145–5159, Nov. 2021.

[19] Y. Ivanenko, V. T. Vu, A. Batra, T. Kaiser, and M. I. Pettersson, "Interpolation methods with phase control for backprojection of complex-valued SAR data," *Sensors*, vol. 22, no. 13, p. 4941, Jun. 2022.

[20] V. T. Vu, T. K. Sjogren, and M. I. Pettersson, "On synthetic aperture radar azimuth and range resolution equations," *IEEE Trans. Aerosp. Electron. Syst.*, vol. 48, no. 2, pp. 1764–1769, Apr. 2012.

VIET T. VU (Senior Member, IEEE) received the Licentiate and Ph.D. degrees in applied signal processing from the Blekinge Institute of Technology (BTH), Sweden, in 2009 and 2011, respectively. Since 2013, he has been with the Department of Mathematics and Natural Sciences, BTH, where he has been a Postdoctoral Researcher in radar algorithm development, an Assistant Professor in radar remote sensing, and currently an Associate Professor in system engineering. He is the author and coauthor of more than 100 scientific publications. His major research interests include SAR signal processing, applications of SAR in change detection and SAR GMTI, and radio occultation.

YEVHEN IVANENKO (Member, IEEE) received the B.Sc. degree in radio electronic devices and the M.Sc. degree in electronic instruments and devices from Odesa National Polytechnic University, Odesa, Ukraine, in 2011 and 2013, respectively, and the M.Sc. degree in electrical engineering and the Ph.D. degree in physics from Linnæus University, Växjö, Sweden, in 2015 and 2021, respectively. Since 2020, he has been a Postdoctoral Researcher with the Systems Engineering Group, Department of Mathematics and Natural Sciences, Blekinge Institute of Technology (BTH), Karlskrona, Sweden. His research interests include SAR signal processing, high-resolution SAR imaging, electromagnetic scattering and absorption, and electromagnetic properties of materials.

MATS I. PETTERSSON (Senior Member, IEEE) received the M.Sc. degree in engineering physics, the Licentiate degree in radio and space science, and the Ph.D. degree in signal processing from the Chalmers University of Technology, Gothenburg, Sweden, in 1993, 1995, and 2000, respectively. He was with Mobile Communication Research at Ericsson, Lund, Sweden. He was also with the Swedish Defense Research Agency (FOI), for ten years. At FOI, he focused on ultrawideband low-frequency SAR systems. Since 2005, he has been with the Blekinge Institute of Technology (BTH), Karlskrona, Sweden, where he is currently a Full Professor, the Research Director, and a member of the BTH Board of Governors. His work is related to remote sensing. His main research interests include SAR inversion and processing, space-time adaptive processing (STAP), high-resolution SAR change detection, automotive radar, and radio occultation.